Dielectric Transitions

Deutsche Ausgabe: DOI: 10.1002/ange.201602028
Internationale Ausgabe: DOI: 10.1002/anie.201602028

Predicting and Screening Dielectric Transitions in a Series of Hybrid Organic–Inorganic Double Perovskites via an Extended Tolerance Factor Approach

*Chao Shi, Chun-Hua Yu, and Wen Zhang**

Abstract: *Extended Goldschmidt tolerance factor t is applied to the hybrid double perovskites $(MA)_2[B'B''(CN)_6]$ (MA = methylammonium cation) to predict and screen dielectric transitions in 121 compounds through the correlations among t, the radius of the B component r_B and the transition temperature T_c, based on experimental results from model compounds. For $(MA)_2[B'Co(CN)_6]$, it is concluded that: i) when $t > 0.873$, the cubic phase would be stable below 298 K; ii) when $0.873 > t > 0.805$, the cubic phase would be stable between 298 and 523 K; iii) the larger the r_B, the higher the T_c of the perovskite ($T_c^{1/2} \propto r_B$); and iv) the T_c of the hybrid perovskites can be well tuned by doping the B components.*

To predict and design solid-state materials with specific properties is one of the central goals in chemistry and materials science. Much effort has been devoted to this direction such as the bottom-up strategy that exploits well-defined building-blocks and/or supramolecular synthons[1,2] and the materials genome approach that relies primarily on high-throughput computational design.[3] Although these practices have already achieved great successes, their further developments and applications are still facing great challenges mainly from the establishment of explicit structure–property relationships which needs deep understandings of the related physical problems in real solid materials.[3e] In this sense, semi-empirical rules that are extracted from experimental facts of series of compounds are still highly effective to guide the prediction and design of desired properties in particular structures.

Dielectric transition or switchable dielectric constant is a structural phase transition-triggered property and corresponds to a dielectric switching between low- and high-dielectric states because of the motional changes of polar components between static and dynamic phases.[4] Molecular materials with dielectric transitions are a type of stimuli-responsive materials and would find potential applications in smart devices as switches, sensors, actuators and so on.[5,6] Recently, we have revealed the switchable dielectric behaviors in hybrid organic-inorganic double perovskites $A_2[B'B''(CN)_6]$ where A is the polar organic cation, B′ is the alkali metal ion and B″ is the trivalent Fe or Co ion.[4a–d] In this type of compounds, the characteristic anionic $[B'_4B''_4(CN)_{12}]$ host cage exerts internal (chemical) pressure on the dynamical changes of the polar guests that are directly associated to the occurrence of the dielectric transition. It is supposed that the explicit relationship between the perovskite structure and the dielectric transition property, especially the transition temperature (T_c), in these materials can be well established. Herein we report a study on the prediction and screening of dielectric transitions in a series of hybrid organic-inorganic double perovskites via an extended tolerance factor approach. Extension of the semi-empirical tolerance factor (t) to the hybrid organic-inorganic perovskites is firstly addressed. Correlations among the T_c, t and ionic radius (r) in hybrid double perovskites are then established and applied, based on the experimental results from model compounds.

In recent years, hybrid organic–inorganic perovskites, as a large family of solid-state compounds related to the inorganic perovskites[7] with ABX_3 stoichiometry in which A is the molecular cation, B is the metal cation and X is the anionic bridging ligand (e.g. halide ion, cyanide, formate, azide, etc.), have drawn much attention because of their rich photovoltaic, conducting, optical, electrical and magnetic properties, together with easy processibility and cheapness.[8–13] When taking the ABX_3 as a structural module, expansion of the ABX_3 to $(ABX_3)_n$ can be made by a sequence-controlled manner like that in polymers,[14] covering the most extensively studied single perovskites ($n = 1$), commonly known as perovskites, double perovskites ($n = 2$), triple perovskites ($n = 3$) and up to n-tuple perovskites (Scheme 1 a). The tolerance factor t, introduced first by Goldschmidt,[15] is mostly used to define the stability of the ideal cubic phase (undistorted phase, $t = 1$) and evaluate the degree of the distortion deviated from the cubic phase (Scheme 1 b). It is naturally modified for the use in inorganic

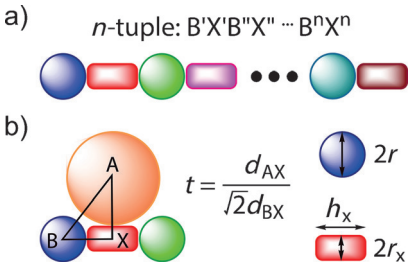

Scheme 1. a) Expansion of the perovskites. For simplicity, the A component is omitted and the packing of the BX_3 modules is illustrated only in one dimension; b) Definition of the Goldschmidt tolerance factor t as a ratio of two distances. The A and B components are described by the effective crystal radius r while the X component is treated as a rigid cylinder ($2r_X * h_X$).

[*] C. Shi, C.-H. Yu, Prof. W. Zhang
Ordered Matter Science Research Center, Southeast University
Nanjing 211189, Jiangsu (China)
E-mail: zhangwen@seu.edu.cn

Supporting information for this article can be found under: http://dx.doi.org/10.1002/anie.201602028.

double perovskites.[16] Very recently, Kieslich and Cheetham extend the factor to hybrid single perovskites.[17] Further extension is herein made in a similar way to the hybrid *n*-tuple perovskites (Table S1). In the case of hybrid double perovskites $A_2B'B''X_6$, the *t* is formulated as

$$t = \sqrt{2}\,(r_A + r_X)/(r_{B'} + r_{B''} + h_X) \quad (1)$$

where *r* is the effective radius of A, B or X (cross section) and *h* is the effective height of the rigid cylinder of X.

It is known that structural phase transitions in the hybrid perovskites are diverse, which are caused by tiltings and distortions of the anionic octahedra, displacements and/or ordering–disordering of the A and B ions.[18] The complicated structural origins pose great challenges for predicting and screening phase transition-triggered properties. Fortunately, when focusing on the cubic-distorted phase transition, the *t* becomes a good descriptor to quantitatively describe the lattice distortions that are driven by interionic bond strains. In this communication, we focus on the hybrid double perovskites $(MA)_2[B'B''(CN)_6]$ (MA = methylammonium cation) to show the correlations among the T_c, *t* and r_B. Three model compounds, i.e., B′/B″ = Na/Co for **1**, K/Co for **2** and Rb/Co for **3**, were synthesized and experimentally characterized.

Compounds **1**–**3** were block-like crystals and keep stable till the onset of thermal decompositions above 530 K (Figure S1 in the Supporting Information). Differential scanning calorimetry (DSC) measurements show **1**–**3** undergo reversible phase transitions at 200 K (T_{c1}) and 260 K (T_{c2}) for **1**, 423 K for **2** and 485 K for **3** (Figure 1 a and S2). The calculated entropy changes ΔS are 18.8 $J\,mol^{-1}\,K^{-1}$ at 200 K and 15.5 $J\,mol^{-1}\,K^{-1}$ at 260 K for **1**, 47.7 $J\,mol^{-1}\,K^{-1}$ for **2**, and 40.2 $J\,mol^{-1}\,K^{-1}$ **3**, indicating that the phase transitions are of the order-disorder type. Meanwhile, IR and/or Raman spectra were measured on **1**–**3** (Figure S3). The characteristic C≡N and N–H vibrations centered around 2120 and 3180 cm^{-1}, respectively, are relatively sharp and/or split in the low-temperature phase (LTP) and become broad and/or merged in the high-temperature phase (HTP).[19] These changes indicate the local environments around the groups are distinguishable in the LTP and indistinguishable in the HTP because of rotation-induced averaged field, corresponding to the order-disorder transitions of the crystals.

Dielectric constant measurements on crystal samples of **1**–**3** show striking dielectric transitions between the high and low states at 250 K for **1**, 423 K for **2** and 485 K for **3**, respectively, consistent with the DSC data (Figure 1 b and S4). At 1 MHz, the three compounds have the same values of dielectric constant ε' (the real part of ε, $\varepsilon = \varepsilon' - i\varepsilon''$) of about 6 in the low-dielectric state while in the high-dielectric state, the ε' values of **1**–**3** are obviously different, i.e., about 24 for **1**, 21 for **2** and 20 for **3**. Another feature of the dielectric transitions is the rapid changes of the dielectric constant around the transition points, indicating a sharp switching property. Higher-frequency dielectric responses of **1** and **2** were also studied in the range 1–1640 MHz (Figure S5). With the increase of the frequency, both the values of ε' and the changes of ε' between the two phases gradually decrease. From the ε'-frequency curves, it is found the ε' values of the HTP decrease quickly above 10 MHz, indicating the frequency of the electric field begins to be comparable with the reorientational rate of the dipoles.

The phase transitions in **1**–**3** were structurally analysed by variable-temperature X-ray diffraction. Taking **2** for example, in the HTP (463 K), it crystallizes in the cubic space group $Fm\bar{3}m$ with $a = b = c = 11.454(6)$ Å, showing an ideal double-perovskite structure (Figure 2 a). In the anionic cage $[K_4Co_4(CN)_{12}]$, the MA cation shows a highly orientational disorder. This is very similar to the well-studied $(MA)(PbI_3)$ perovskite in the HTP where there are three major models for the possible configurations of the MA cation in the anionic cage: i) face ([100] orientations); ii) edge ([110] orientations); and iii) corner ([111] orientations).[20] The model (i) is adopted in **2** and the indistinguishable C and N atoms are refined as N atom. Besides the highly orientationally disordered MA

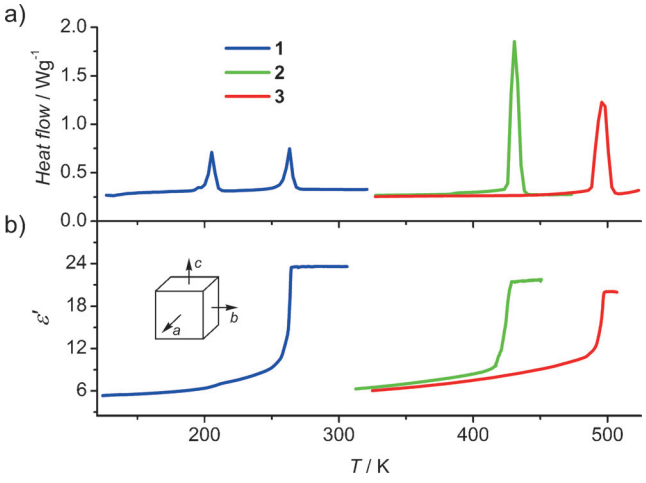

Figure 1. a) DSC curves upon heating and b) the real part of dielectric constant measured at 1 MHz on single crystals along the <100> direction of the cubic phase of **1**–**3**.

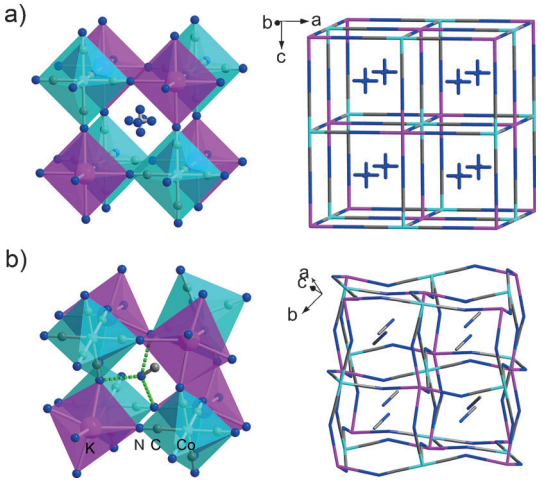

Figure 2. Cages and packing structures of **2** in the a) HTP and b) LTP. The highly disordered MA cation in the HTP is refined as N atom. Hydrogen atoms are omitted for clarity. Dotted lines represent hydrogen bonds.

cations, thermal oscillations of the rigid $Co(CN)_6$ are evidenced by the large anisotropic thermal vibrations of the N atoms of the CN groups (Table S5). In the LTP (293 K), **2** shows a drastic structure change by adopting the monoclinic space group *C*2/*c*. The cells of the HTP and LTP are related by a transformation matrix (Figure S6). The highly distorted version of the perovskite structure is characterized by the tilting of the rigid $Co(CN)_6$ unit, distortion of the relatively labile KN_6 octahedron, displacement of the K ion and the totally ordered MA cation (Figure 2b). The anionic cage $[K_4Co_4(CN)_{12}]$ becomes irregular in which the MA cation is anchored by weak hydrogen bonds between the NH_3 and CN groups (Table S4). It is noted that the polar MA cations in the lattices show the characteristic paraelectric- and antiferroelectric-like arrays in the HTP and LTP, respectively, which would give a hint to settle the dispute on the ferroelectricity in $(MA)(PbX_3)$ (Figure S7).[21] Compounds **1** and **3** adopt $Fm\bar{3}m$ and *C*2/*c* space group, respectively, at 293 K (Figure S8, S9 and Table S2). Unfortunately. theirs structures after phase transitions cannot be obtained. The two compounds are supposed to undergo similar structure changes to **2** between the ideal cubic and distorted phases, abiding by the general rule of temperature-dependent symmetry changes in perovskite structures (Figure S10).[8,22] For example, the cell parameters of **1** in the intermediate-temperature phase (213 K) are indexed as $a = 10.944(4)$ Å, $b = 10.944(4)$ Å, $c = 10.975(6)$ Å, and $\alpha = \beta = \gamma = 90°$ with a primitive tetrahedral system.

Based on above measurements and theory of dielectrics, the dielectric transitions in **1**–**3** can be well explained.[23] In the low-dielectric state, the polar MA cations are totally ordered and make no contribution to the dielectric constant. Around the T_c, the MA cations become disordered by undergoing dipolar reorientational rotations, corresponding to a static–motional transition. This type of dynamic changes have been revealed in the attracting perovskite analogues $(MA)(PbX_3)$ (X = halide).[20b,24] With the contribution of the dipolar reorientations, the ε' values jump to the high-dielectric state. For **1**, it shows an additional small dielectric change of about 1.3 at $T_{c1} = 200$ K that is supposed to come from structural rearrangement of the anionic framework. A further solid-state NMR study on the local dynamic changes of the MA cations and the octahedral anions is now under way.

It is clear that in **1**–**3** the dielectric transition that is triggered by the cubic-distorted phase transition can be described by the tolerance factor. For the hybrid double perovskites $(MA)_2[B'B''(CN)_6]$, Equation (1) is expressed as:

$$t = 513.283/(r_{B'} + r_{B''} + 395) \quad (2)$$

by adopting the effective radii from Shannon[25] and Kieslich and Cheetham.[17,26] With the combination of 11 B′(I) and 11 B″(III) metal ions, the t values of 121 compounds are calculated, being 0.886, 0.834 and 0.815, respectively, for **1**–**3** (Figure 3a, S11 and Table S6). Furthermore, a linear relationship between the $r_{B'}$ and $T_c^{1/2}$,

$$r_{B'} = -19.53 + 8.39T_c^{1/2} \quad (3)$$

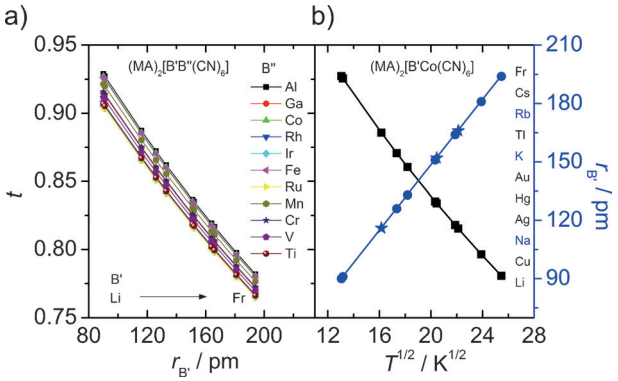

Figure 3. a) Tolerance factors of $(MA)_2[B'B''(CN)_6]$; b) Plots of t and $r_{B'}$ versus $T^{1/2}$ for $(MA)_2[B'Co(CN)_6]$. The t is calculated from Equation (2) and correlated to the T from the linear fitting between $r_{B'}$ and $T^{1/2}$. The star symbols represent the experimental data of **1**–**3**. Lines are guide for the eye.

is fitted on the experimental data of **1**–**3** (Figure S12). It is based on the fact that the T_c is proportional to bond-strain energy ΔU_s which triggers the cubic-to-distorted phase transition while the ΔU_s is proportional to $(d_{BX} - d_{AX}/\sqrt{2})^2$ where $d_{BX} = 0.5 \times (r_{B'} + r_{B''} + h_X)$ (Scheme 1b).[27] Thus, the relationship between the t and $T_c^{1/2}$ can be derived from Equations (2) and (3) (Figure 3b).

From these results, it is concluded that: i) when $t > 0.873$, the cubic phase would be stable below 298 K; ii) when $0.873 > t > 0.805$, the cubic phase would be stable between 298 and 523 K (assumed decomposition temperature); iii) the larger the r_B, the higher the T_c of the perovskite ($T_c^{1/2} \propto r_B$); and iv) the T_c of the hybrid perovskites can be well tuned by doping the B components.[11e] Considering the B″ = Fe series, they should show very similar phase transition behaviors because of the very close $r_{B''}$ values, i.e., 69 pm for Fe and 68.5 pm for Co. For example, the T_c of the cubic-monoclinic phase transition in $(MA)_2[KFe(CN)_6]$ is 426 K, about 3 K higher than **2**, and it would be around 263 K in $(MA)_2[NaFe(CN)_6]$.[28]

Future studies of the extended tolerance factor approach would include: i) to thoroughly understand the phase transition mechanism; ii) to explore the limitations and applicability of the approach; iii) to apply to other A, B and X combinations as a general approach to predict and screen new hybrid perovskite materials with particular properties; and iv) to predict phase separation to guide the fabrication of homo- or hetero-structure perovskites via doping or layer-by-layer assembly to tune the structures and functionalities of the hybrid perovskites.[8,26]

In summary, the extended Goldschmidt tolerance factor t is applied to the hybrid double perovskites $(MA)_2[B'B''(CN)_6]$ to predict and screen dielectric transitions in 121 compounds through the correlations among the t, the radius of the B component and the transition temperature, based on experimental results from $(MA)_2[B'Co(CN)_6]$ (B′ = Na, K, Rb). Such a success roots on the explicit relationship between the dielectric transition and the cubic-distorted phase transition which is triggered by octahedral tiltings in the perovskite structures because of bond-strain energy. Notably,

the series of compounds resembles the star compound $(MA)(PbX_3)$. Considering their structural diversity and rich electrical properties, the hybrid organic-inorganic double perovskites would find roles in the exploration of promising organic–inorganic electronic and photovoltaic materials.

Acknowledgements

This work was financially supported by NSFC (Grant No. 21225102).

Keywords: dielectric transition · hybrid double perovskite · phase transition · switchable dielectric constant · tolerance factor

How to cite: *Angew. Chem. Int. Ed.* **2016**, *55*, 5798–5802
Angew. Chem. **2016**, *128*, 5892–5896

[1] a) O. M. Yaghi, M. O'Keeffe, N. W. Ockwig, H. K. Chae, M. Eddaoudi, J. Kim, *Nature* **2003**, *423*, 705; b) H. C. Zhou, J. R. Long, O. M. Yaghi, *Chem. Rev.* **2012**, *112*, 673.

[2] a) G. R. Desiraju, *Crystal Engineering: the Design of Organic Solids*, Elsevier, Amsterdam, **1989**; b) G. R. Desiraju, *Angew. Chem. Int. Ed. Engl.* **1995**, *34*, 2311; *Angew. Chem.* **1995**, *107*, 2541.

[3] a) C. M. Draznieks, J. M. Newsam, A. M. Gorman, C. M. Freeman, G. Férey, *Angew. Chem. Int. Ed.* **2000**, *39*, 2270; *Angew. Chem.* **2000**, *112*, 2358; b) C. Mellot-Draznieks, J. Dutour, G. Férey, *Angew. Chem. Int. Ed.* **2004**, *43*, 6290; *Angew. Chem.* **2004**, *116*, 6450; c) S. M. Woodley, R. Catlow, *Nat. Mater.* **2008**, *7*, 937; d) A. Jain, S. P. Ong, G. Hautier, W. Chen, W. D. Richards, S. Dacek, S. Cholia, D. Gunter, D. Skinner, G. Ceder, K. A. Persson, *APL Mater.* **2013**, *1*, 011002; e) S. Curtarolo, G. L. W. Hart, M. B. Nardelli, N. Mingo, S. Sanvito, O. Levy, *Nat. Mater.* **2013**, *12*, 191.

[4] a) W. Zhang, Y. Cai, R.-G. Xiong, H. Yoshikawa, K. Awaga, *Angew. Chem. Int. Ed.* **2010**, *49*, 6608; *Angew. Chem.* **2010**, *122*, 6758; b) W. Zhang, H.-Y. Ye, R. Graf, H. W. Spiess, Y.-F. Yao, R.-Q. Zhu, R.-G. Xiong, *J. Am. Chem. Soc.* **2013**, *135*, 5230; c) X. Zhang, X.-D. Shao, S.-C. Li, Y. Cai, Y.-F. Yao, R.-G. Xiong, W. Zhang, *Chem. Commun.* **2015**, *51*, 4568; d) C. Shi, X. Zhang, Y. Cai, Y.-F. Yao, W. Zhang, *Angew. Chem. Int. Ed.* **2015**, *54*, 6206; *Angew. Chem.* **2015**, *127*, 6304; e) X.-D. Shao, X. Zhang, C. Shi, Y.-F. Yao, W. Zhang, *Adv. Sci.* **2015**, *2*, 1500029.

[5] a) *Handbook of Stimuli-Responsive Materials* (Ed.: M. W. Urban), Wiley-VCH, Weinheim, **2011**; b) P. Theato, B. S. Sumerlin, R. K. O'Reilly, T. H. Epps III, *Chem. Soc. Rev.* **2013**, *42*, 7055; c) O. Sato, J. Tao, Y.-Z. Zhang, *Angew. Chem. Int. Ed.* **2007**, *46*, 2152; *Angew. Chem.* **2007**, *119*, 2200.

[6] Y. S. Kim, M. Liu, Y. Ishida, Y. Ebina, M. Osada, T. Sasaki, T. Hikima, M. Takata, T. Aida, *Nat. Mater.* **2015**, *14*, 1002.

[7] a) F. S. Galasso, *Structure, Properties and Preparation of Perovskite Type Compounds*, Pergamon Press, Oxford, **1969**; b) *Properties and Applications of Perovskite Type Oxides* (Eds.: L. J. Tejuca, J. L. G. Fierro), Marcel Dekker, New York, **1993**; c) F. Jona, G. Shirane, *Ferroelectric Crystals*, Pergamon Press, New York, **1962**; d) C. N. R. Rao, B. Raveau, *Colossal Magnetoresistance, Charge Ordering and Related Properties of Manganese Oxides*, World Scientific, Singapore, **1998**; e) A. R. Akbashev, A. R. Kaul, *Russ. Chem. Rev.* **2011**, *80*, 1159.

[8] D. B. Mitzi, C. A. Feild, W. T. A. Harrison, A. M. Guloy, *Nature* **1994**, *369*, 467.

[9] a) A. Kojima, K. Teshima, Y. Shirai, T. Miyasaka, *J. Am. Chem. Soc.* **2009**, *131*, 6050; b) J. Burschka, N. Pellet, S.-J. Moon, R. Humphry-Baker, P. Gao, M. K. Nazeeruddin, M. Grätzel, *Nature* **2013**, *499*, 316; c) M. Liu, M. B. Johnston, H. J. Snaith, *Nature* **2013**, *501*, 395; d) S. Kazim, M. K. Nazeeruddin, M. Grätzel, S. Ahmad, *Angew. Chem. Int. Ed.* **2014**, *53*, 2812; *Angew. Chem.* **2014**, *126*, 2854.

[10] a) B. Kundys, A. Lappas, M. Viret, V. Kapustianyk, V. Rudyk, S. Semak, C. Simon, I. Bakaimi, *Phys. Rev. B* **2010**, *81*, 224434; b) A. O. Polyakov, A. H. Arkenbout, J. Baas, G. R. Blake, A. Meetsma, A. Caretta, P. H. M. van Loosdrecht, T. T. M. Palstra, *Chem. Mater.* **2012**, *24*, 133; c) W.-Q. Liao, Y. Zhang, C.-L. Hu, J.-G. Mao, H.-Y. Ye, P.-F. Li, S. D. Huang, R.-G. Xiong, *Nat. Commun.* **2015**, *6*, 7338.

[11] a) X.-Y. Wang, L. Gan, S.-W. Zhang, S. Gao, *Inorg. Chem.* **2004**, *43*, 4615; b) P. Jain, N. S. Dalal, B. H. Toby, H. W. Kroto, A. K. Cheetham, *J. Am. Chem. Soc.* **2008**, *130*, 10450; c) P. Jain, V. Ramachandran, R. J. Clark, H. D. Zhou, B. H. Toby, N. S. Dalal, H. W. Kroto, A. K. Cheetham, *J. Am. Chem. Soc.* **2009**, *131*, 13625; d) S. Chen, R. Shang, K. L. Hu, Z. M. Wang, S. Gao, *Inorg. Chem. Front.* **2014**, *1*, 83; e) S. Chen, R. Shang, B.-W. Wang, Z.-M. Wang, S. Gao, *Angew. Chem. Int. Ed.* **2015**, *54*, 11093; *Angew. Chem.* **2015**, *127*, 11245.

[12] a) X.-H. Zhao, X.-C. Huang, S.-L. Zhang, D. Shao, H.-Y. Wei, X.-Y. Wang, *J. Am. Chem. Soc.* **2013**, *135*, 16006; b) Z.-Y. Du, T.-T. Xu, B. Huang, Y.-J. Su, W. Xue, C.-T. He, W.-X. Zhang, X.-M. Chen, *Angew. Chem. Int. Ed.* **2015**, *54*, 914; *Angew. Chem.* **2015**, *127*, 928.

[13] D. B. Mitzi, *Prog. Inorg. Chem.* **1999**, *48*, 1.

[14] *Sequence-Controlled Polymers: Synthesis Self-Assembly, and Properties*, *Vol. 1170*, American Chemical Society, Washington, **2014**.

[15] V. M. Goldschmidt, *Naturwissenschaften* **1926**, *14*, 477.

[16] a) D. Babel, R. Haegele, G. Pausewang, F. Wall, *Mater. Res. Bull.* **1973**, *8*, 1371; b) A. Gormezano, M. T. Weller, *J. Mater. Chem.* **1993**, *3*, 979.

[17] a) G. Kieslich, S. Sun, A. K. Cheetham, *Chem. Sci.* **2014**, *5*, 4712; b) G. Kieslich, S. Sun, A. K. Cheetham, *Chem. Sci.* **2015**, *6*, 3430.

[18] a) A. M. Glazer, *Acta Crystallogr. Sect. B* **1972**, *28*, 3384; b) P. M. Woodward, *Acta Crystallogr. Sect. B* **1997**, *53*, 32; P. M. Woodward, *Acta Crystallogr. Sect. B* **1997**, *53*, 44; c) I. N. Flerov, M. V. Gorev, K. S. Aleksandrov, A. Tressaud, J. Grannec, M. Couzi, *Mater. Sci. Eng. R* **1998**, *24*, 81; d) K. S. Aleksandrov, J. Bartolomé, *Phase Transitions* **2001**, *74*, 255; e) M. C. Knapp, P. M. Woodward, *J. Solid State Chem.* **2006**, *179*, 1076; f) G. King, P. M. Woodward, *J. Mater. Chem.* **2010**, *20*, 5785.

[19] a) T. Glaser, C. Müller, M. Sendner, C. Krekeler, O. E. Semonin, T. D. Hull, O. Yaffe, J. S. Owen, W. Kowalsky, A. Pucci, R. Lovrinčić, *J. Phys. Chem. Lett.* **2015**, *6*, 2913; b) C. Quarti, G. Grancini, E. Mosconi, P. Bruno, J. M. Ball, M. M. Lee, H. J. Snaith, A. Petrozza, F. De Angelis, *J. Phys. Chem. Lett.* **2014**, *5*, 279; c) M. Sánchez-Andújar, S. Presedo, S. Yáñez-Vilar, S. Castro-García, J. Shamir, M. A. Señarís-Rodríguez, *Inorg. Chem.* **2010**, *49*, 1510.

[20] a) H. Mashiyama, Y. Kawamura, H. Kasano, T. Asahi, Y. Noda, H. Kimura, *Ferroelectrics* **2007**, *348*, 182; b) A. M. A. Leguy, J. M. Frost, A. P. McMahon, V. G. Sakai, W. Kockelmann, C. Law, X. Li, F. Foglia, A. Walsh, B. C. O'Regan, J. Nelson, J. T. Cabral, P. R. F. Barnes, *Nat. Commun.* **2015**, *6*, 7124.

[21] a) J. M. Frost, K. T. Butler, F. Brivio, C. H. Hendon, M. van Schilfgaarde, A. Walsh, *Nano Lett.* **2014**, *14*, 2584; b) J. Wei, Y. Zhao, H. Li, G. Li, J. Pan, D. Xu, Q. Zhao, D. Yu, *J. Phys. Chem. Lett.* **2014**, *5*, 3937; c) Z. Fan, J. Xiao, K. Sun, L. Chen, Y. Hu, J. Ouyang, K. P. Ong, K. Zeng, J. Wang, *J. Phys. Chem. Lett.* **2015**, *6*, 1155; d) Z. Xiao, Y. Yuan, Y. Shao, Q. Wang, Q. Dong, C. Bi, P. Sharma, A. Gruverman, J. Huang, *Nat. Mater.* **2015**, *14*, 193.

[22] a) C. J. Howard, B. J. Kennedy, P. M. Woodward, *Acta Crystallogr. Sect. B* **2003**, *59*, 463; b) C. J. Howard, H. T. Stokes, *Acta Crystallogr. Sect. A* **2005**, *61*, 93.
[23] H. Fröhlich, *Theory of Dielectrics*, 2nd ed., Oxford University Press, Oxford, **1965**.
[24] a) R. E. Wasylishen, O. Knop, J. B. Macdonald, *Solid State Commun.* **1985**, *56*, 581; b) N. Onoda-Yamamuro, T. Matsuo, H. Suga, *J. Phys. Chem. Solids* **1992**, *53*, 935.
[25] R. D. Shannon, *Acta Crystallogr. Sect. A* **1976**, *32*, 751.
[26] D. B. Mitzi, *J. Chem. Soc. Dalton Trans.* **2001**, 1.
[27] a) N. M. Olekhnovich, *Crystallogr. Rep.* **2006**, *51*, 169; b) N. M. Olekhnovich, *Crystallogr. Rep.* **2005**, *50*, 435.
[28] a) W.-J. Xu, S.-L. Chen, Z.-T. Hu, R.-B. Lin, Y.-J. Su, W.-X. Zhang, X.-M. Chen, *Dalton Trans.* **2016**, *45*, 4224; b) S. Peschel, D. Babel, *Z. Naturforsch. B* **1994**, *49*, 1373.

Received: February 26, 2016
Published online: April 6, 2016

